Spatial and voxel-wise evaluation of eigenvector stability within the human calf at 3T

Conrad Rockel[1,2] and Michael D Noseworthy[1,2]

[1]*School of Biomedical Engineering, McMaster University, Hamilton, Ontario, Canada,* [2]*Imaging Research Centre, St Joseph's Healthcare, Hamilton, Ontario, Canada*

Target Audience: Clinicians and researchers using DTI to examine biomechanical properties of skeletal muscle.

Background: Diffusion tensor imaging (DTI) can be used to quantify tissue characteristics, based the self-diffusion of water through tissue. Because the principal vector of diffusion has been found to correlate with fibers in directional tissue[1,2], this technique is gaining popularity in the study of skeletal muscle[3,4]. Studies suggest that the elliptical cross-sections of muscle fibers[5] are quantifiable using DTI[3], and that DTI eigenvalues may be of use in *in-vivo* biomechanical studies of skeletal muscle[4]. However, the stability of the eigenvectors associated with these eigenvalues is rarely reported. Principal eigenvector (V1) stability has been addressed in simulations[6,7,8], although it has been noted that brain results may not apply to muscle[9], and that simulation results may differ from real data[8,9].

Purpose: To use *in vivo* human skeletal muscle DTI data to visualize spatial regions of eigenvector variability, compare variability between the three eigenvectors, determine impact of different gradient schemes and number of signal averages (NSA) on vector variability, and examine how variability of V1 impacts the second eigenvector (V2).

Methods: The widest cross section of the right calf of 4 healthy volunteers (mean age = 25.1+/-4.7 yoa) was evaluated using a GE MR750 3T and an 8-channel lower extremity coil (GE Healthcare, Milwaukee WI). DTI data was acquired using a dual echo spin echo EPI sequence (b=400s/mm^2, TR/TE=6000/70ms, gradient schemes = 6, 15, or 25 directions, 16 slices 4mm thick, 16cm FOV, 64x64, ASSET = 2). Nine individual signal averages (NSA) were collected for each gradient scheme per subject in randomized order. DTI data were preprocessed by combining volumes of 3, 2, or 1 NSA. Eigenvectors of each combination were then calculated using FSL[10]. The majority of skin and subcutaneous fat was removed from each volume using BET[10]. Voxel-wise differences in eigenvector orientation were calculated in degrees for each pair of volumes per 3-volume set[11], and subsequently averaged. Spatial maps of mean vector variation were then produced using Matlab (Mathworks, Natick MA) for each combination of gradient scheme and NSA, per subject. Histograms of mean vector difference in degrees were generated to assess voxel-wise distribution of variability for each eigenvector, allowing comparison across 4 volunteers, as well as between the 3 eigenvectors. To assess the variability of V2 per V1, the histogram of mean V1 variability for '25dir, 3 NSA' was divided based on degrees variability. Regions of interest (ROIs) were created for each subject in each condition based on V1 variability. The ROIs corresponding to the 3 categories of least V1 variability were applied to spatial maps of V2 variability to assess V2 distribution according to V1. Histograms of V2-via-V1 were normalized per subject according to area under the curve, and averaged between subjects. Finally, signal-to-noise ratio (SNR) maps were calculated for the b=0 image of each volume set in order to assess the impact of SNR on vector stability on a voxel-wise basis[12].

Results: V1 appeared to vary in a non-random manner, and seemed to be minimal in mid-regions of peripheral muscles of the calf (gastrocnemius, anterior tibialis). The soleus demonstrated increased variation, even in areas closer to peripheral calf regions **[Fig.1]**. V2 and V3 variability appeared to have similar spatial distributions, though noisier. Histograms showed a range 0-180^O, with a broad peak between 0-20 ^{O}, spike at 90 ^{O}, and lesser "mirror peak" at 160-180^O. Spikes at 90 degrees occurred in locations of masking mismatch, an artifact determined using the spatial maps. Additionally, the "mirror region" (>90^O) appeared to be concentrated in the central calf region as well as throughout the soleus. The distributions of V2 and V3 appeared remarkably different than V1, with lower initial peak, more voxels of high vector variability, and higher "mirror" peaks **[Fig.2]**. Increasing the number of gradient directions and NSA served to increase and narrow the initial peak of all histograms **[Fig.3]**. Comparison of histograms appeared related to overall condition scan time[13], although this relationship weakened for V2 and V3. Histograms of V2 variability displayed 0-180^O range regardless of V1 variability. However, distributions of V2-via-V1 variability appeared somewhat stable, with peaks of V2 akin to categories of V1 **[Fig.4]**. Finally, it seemed that NSA provoked more differences in normalized distributions of V2 variability by V1 than did gradient scheme. The distribution of vector precision seemed to be largely influenced by SNR, although the relationship was not straightforward, as higher SNR peaks of greater volume were found to occur in schemes involving fewer directions.

Discussion: Spatial mapping of vector variability allows (i) identification of appropriate anatomical regions for use of eigenvalues in physiological or biomechanical studies of skeletal muscle; (ii) explanation of anomalous vector variation; and (iii) demonstration of the relationship between variability of the principal eigenvector and minor eigenvector stability within *in-vivo* studies. Future studies will need to consider fiber vascularity and orientation in order to further assess stability of the eigenvectors.

References: **[1]** Moseley ME et al. Radiology 1990; 176:439-45. **[2]** van Donkelaar CC et al. *J Anat* 1999; 194:79-88. **[3]** Galban C et al. *Eur J Appl Physiol 2004*; 93(3):256-62. **[4]** Schwenzer NF et al. *NMR Biomed* 2009; 22:1047-53. **[5]** Campos GE et al. Eur J Appl Physiol 2002; 85:50-60. **[6]** Jones JK. *Magn Reson Imaging* 2003; 49:7-12. **[7]** Damon B. *Magn Reson Med* 2008; 60(4); 934-44. **[8]** Farrell JAD et al. *J Magn Reson Imaging* 2007; 26:756-767.**[9]** Froeling M et al. *NMR Biomed* 2013. 26:1339-1352. **[10]** http://fsl.fmrib.ox.ac.uk/fsl/. **[11]** Fleisch D. A Student's Guide to Vectors and Tensors. Cambridge University Press, 2012. **[12]** Dietrich O et al. *J Magn Reson Imaging* 2007; 26:375-85. **[13]** Landman BA et al. *NeuroImage* 2007; 36:1123-38.

FIG 1

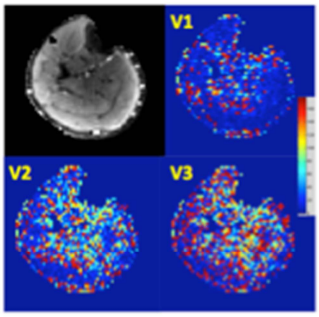

FIG 2

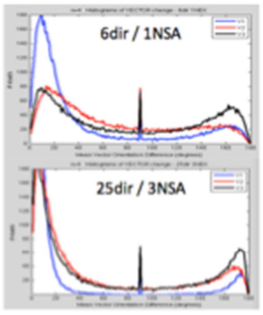

FIG 3

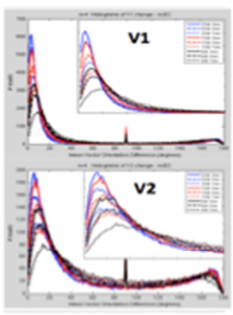

FIG 4